



Support Vector Machines Regression for the Estimation of Forest Stand Parameters Using Airborne Laser Scanning

Jean-Matthieu Monnet, Jocelyn Chanussot, *Senior Member, IEEE*, Frédéric Berger

Abstract—Airborne laser scanning is nowadays widely used for the estimation of forest stand parameters. Prediction models have to deal with high dimensional laser data sets as well as limited field calibration data. This problem is enhanced in mountainous areas where forest is highly heterogeneous and field data collection costly. Artificial neural network models and support vector regression (SVR) have already demonstrated their ability to address such issues for species specific plot volume prediction. In this paper we compare the stand parameters prediction accuracies of support vector machines and ordinary least squares multiple regression models for dominant height, basal area, mean diameter and stem density. Sensitivity of these techniques to the input variables is investigated by testing data sets including different number and types of laser metrics, and by reducing their dimension with principal component and independent component analyzes. Whereas usual variables only reflect the vertical distribution, we also integrate the entropy of the horizontal distribution of the point cloud in the laser metrics. Results show that SVR prediction models are of similar accuracy than multiple regression models, but are more robust regarding the metrics included in the data sets. Preliminary dimension reduction of the data set by principal component analysis generally benefits more to SVR than to multiple regression. The optimal combination of laser metrics to be included in the data sets mainly depends on the forest parameter to be estimated.

Index Terms—Forestry, airborne laser scanning, prediction methods, remote sensing, support vector regression, dimension reduction, entropy.

I. INTRODUCTION

SINCE the end of the 90's, numerous studies have shown the accuracy and efficiency of airborne laser scanning for the extraction of forest stand parameters such as canopy height [1], basal area, volume [2], mean diameter [3] or stem density [4]. One of the widely-used processing method is the so-called area-based method. It was first implemented in Nordic countries [5] and tested since in other contexts such as temperate deciduous stands [6] and alpine environments [7]. It consists in relating forest parameters to several height and density metrics derived from the laser point cloud in fixed areas.

Most of the studies relied on ordinary least squares multiple regression (*ols*-MR) to establish relationships between laser

metrics and forest parameters. A comparison of seemingly unrelated, partial least squares and ordinary least squares regressions showed only minor discrepancies [8]. However, parametric methods reach their limits when dealing with a small number of field observations combined with high dimensional data. Such cases tend to occur frequently when laser scanning data is acquired over mountainous forests. Indeed, lack of accessibility hamper field inventories whereas numerous laser metrics may be extracted from the point cloud. The non parametric *k*-most similar neighbor method has been successfully tested for species-specific stand attributes estimation from laser data [9]. In a comparison with *k*-most similar neighbor and artificial neural network models such as self organizing map and multilayer perceptron, support vector machines regression (SVR) turned out to be one of the best suited method for prediction purposes [10].

Support vector machines (SVM) are a training approach based on the framework of statistical learning theory. They have proved their robustness to dimensionality and generalization abilities [11]. Moreover non-linear relationships can be accounted for thanks to the kernel trick. SVM are now widely used in the field of remote sensing, mainly for the purpose of hyperspectral image processing [12], but also for continuous variables estimation [10], [13]–[16].

In this paper we aim at comparing accuracies of forest stand parameters estimates obtained with *ols*-MR and SVR. Concerning prediction models using laser data, one key issue to avoid over fitted or complex models is the selection of relevant laser metrics. For multiple regression most of the studies relied on stepwise variable selection [4], [6], [7] or exhaustive comparison of combinations [2]. Here we investigated an alternative way by reducing data dimension with principal component analysis (PCA) or independent component analysis (ICA). We also tested the effect of the inclusion of different numbers and types of laser metrics on prediction accuracy and introduced a laser metric calculated as the entropy of the horizontal distribution of the point cloud. Fig. 1 presents the global workflow implemented in this study.

The paper is organized as follows: in Section II, we describe the study area and data used; in Section III, we present the workflow and particularly the constitution of predictors sets by laser metrics extraction and dimension reduction. Experimental results are detailed in Section IV and discussed in Section V. Finally, some conclusive remarks are drawn in Section VI.

Manuscript received Oct. 11, 2010; revised Nov. 9, 2010. J.-M. Monnet holds a doctoral fellowship from région Rhône-Alpes.

J.-M. Monnet and F. Berger are with Cemagref, UR EMGR, F-38402 St-Martin-d'Hères, France (e-mail: jean-matthieu.monnet, frederic.berger@cemagref.fr). J. Chanussot is with GIPSA-Lab, Grenoble Institute of Technology, BP 46, 28402 Saint Martin D'Hères, France.

DOI:

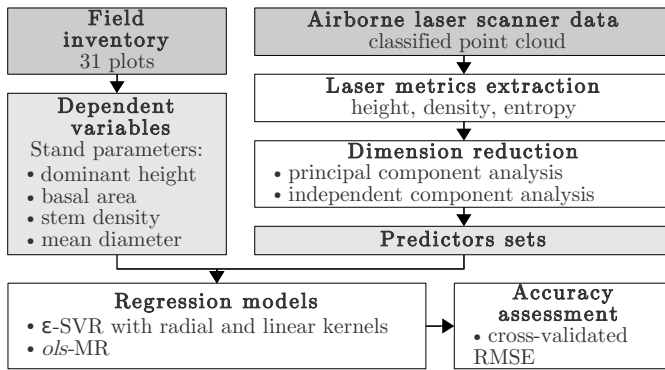


Fig. 1. Flow chart of the methodology implemented in this study.

II. MATERIAL

A. Field data

The study area is a 4 km² hillside located in the French Alps (town of Saint Paul de Varces, 45°04'17"N, 05°38'25"E, see Fig. 2). The forest is mainly constituted of coppice stands and deciduous stands on poor quality sites, dominated by Italian maples (*Acer opalus*) and downy oaks (*Quercus pubescens*). Downslope, old coppice chestnut (*Castanea sativa*) stands are frequent. Common whitebeam is present in all the area, especially at the foot of cliffs. In thalwegs or in the upper parts with better site quality, ash (*Fraxinus excelsior*) and beech (*Fagus sylvatica*) are common. Altitude ranges from 330 to 1270 m above sea level.

From September to November 2009, 31 circular field plots were inventoried. Plots were distributed every 400 m along the 550, 750, 950 and 1150 m height contours, resulting in an irregular sampling scheme where horizontal distances between neighboring plots ranged from 180 to 412 m with a mean value of 302 m. Plot centers were georeferenced using a Trimble GPS Pro XRS receiver. After differential correction with the Pathfinder® software, the position precision (95% confidence radius) ranged from 0.6 to 1.5 m. All trees with diameter at breast height larger than 5 cm and located within 10 m horizontal distance from the plot center had their diameter measured with a tape. Maples (mainly *Acer opalus*), downy oak (*Quercus pubescens*) and common whitebeam (*Sorbus aria*) represented nearly 60 % of the stems. Ten tree heights were measured on each plot using a Vertex III hypsometer. Sampling probability was proportional to stem basal area

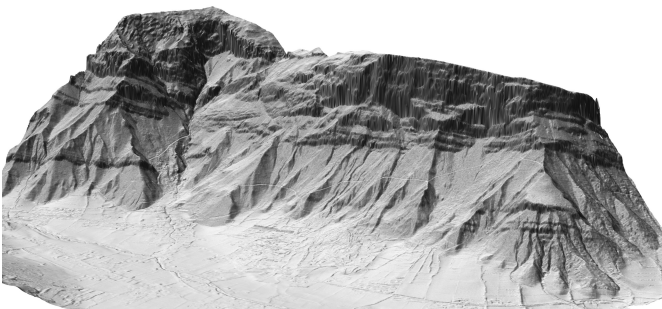


Fig. 2. Shaded digital terrain model of the study area.

TABLE I
FOREST STAND PARAMETERS STATISTICS (31 FIELD PLOTS)

Parameter	H_{dom} (m)	G (m ² .ha ⁻¹)	N_s (ha ⁻¹)	\overline{dbh} (cm)
Mean	17.8	34.8	1735	14.5
Min	8.1	4.6	764	8.3
Max	28.5	59.7	2833	22.7
Std deviation	5.3	11.4	577	3.6

to ensure that dominant trees would be represented. The following forest stand parameters were then computed for each plot: dominant height (H_{dom} : mean height of the 30 highest trees per hectare), basal area (G : surface occupied by the horizontal section of tree stems at 1.30 m height), stem density (N_s) and mean diameter at breast height (\overline{dbh}) (Table I).

B. Laser data

Laser data were acquired on August 27th, 2009 over 8.6 km² with a fullwave RIEGL LMS-Q560 scanner. Laser footprint was 0.3 m and scan angle $\pm 30^\circ$. Average scanning density was 2.8 pulses.m⁻² with 50% overlap between adjacent flight strips. Echos were extracted from the binary acquisition files and georeferenced with the RIEGL software suite. The contractor also classified the resulting point cloud into ground and non-ground echoes using the TerraScan software. Final echo density was 10 m⁻².

III. METHODS

A. Predictors sets

For each plot, laser points within 10 m horizontal distance from the plot center were selected. Their relative heights were computed by subtracting the terrain height at their orthometric coordinates. Terrain surface was estimated by bilinear interpolation of points classified as ground points. Points with relative height lower than 2 m were excluded to avoid influence of dense shrubs understories. Three point groups were then constituted according to return positions: single echoes (only one echo for a given pulse), first echoes and last echoes. For each group, n_h height metrics and n_d density metrics were calculated. The height metrics included the minimum, maximum, mean and q -quantiles of the height distribution (total: $n_h = q + 2$). The density metrics were computed as the proportions of points located below fractions $(\frac{i}{n_d+1})_{i \in \{1, \dots, n_d\}}$ of the maximum height of the point group. Entropy metrics related to the horizontal dispersion of echoes were also calculated. The whole point cloud was horizontally divided in 2 m wide square pixels (s_i) and vertically divided in n_e height bins of equal width $(h_j)_{j \in \{1, \dots, n_e\}}$. For each height bin h_j , the entropy metric is computed as $e_j = \sum_i p_{i,j} \log(p_{i,j})$ with $p_{i,j} = \frac{\text{card}(s_i \cap h_j)}{\text{card}(h_j)}$. A set of independent predictors $(v_i)_{i \in \{1, \dots, n_v\}}$ is thus composed of $n_v = 3 \times (n_h + n_d) + n_e$ laser metrics.

For example, the predictors set $(n_h, n_d, n_e) = (6, 3, 3)$ has 30 laser metrics. For each of the three point groups, six height metrics are calculated (minimum, first quartile, median, third quartile, maximum and mean), and three density metrics (proportion of echoes below 25%, 50% and 75% of the maximum height of the group). Entropy metrics for the whole

TABLE II
BEST PREDICTION ACCURACY OBTAINED WITH *ols*-MR AND ϵ -SVR WITH THE PREDICTORS SETS DERIVED FROM LASER METRICS WITH $(n_h, n_d, n_e) = (6, 3, 3)$, AND CORRESPONDING DIMENSION REDUCTION SETTINGS.

	<i>ols</i> -MR			ϵ -SVR		
	CV_{RMSE} (%)	Model predictors	Dimension reduction and number of components	CV_{RMSE} (%)	Kernel	Dimension reduction and number of components
Dominant height	12.6	3	none	10.1	linear	none
Basal area	18.7	3	ICA-14	20.4	linear	none
Stem density	23.6	2	none	18.4	linear	PCA-30
Mean diameter	14.6	3	none	16.1	radial	PCA-3

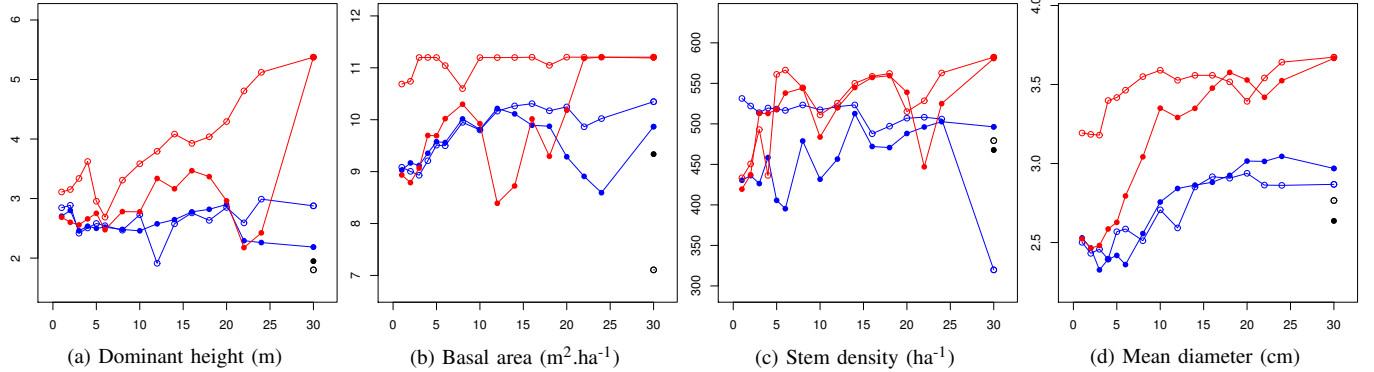


Fig. 3. Root mean square error of the estimation of each stand parameter plotted against the number of predictors in the model. Predictors sets are derived from $(n_h, n_d, n_e) = (6, 3, 3)$ and RMSE is computed by leave-one-out cross validation. Symbol types refer to the kernel used in ϵ -SVR: linear (\circ) or radial (\bullet). Symbol colors refer to the method used for dimension reduction: PCA (blue), ICA (red) or none (black).

point cloud are calculated as the entropies of the horizontal distribution of echoes located in three height bins: $[0, \frac{h}{3}]$, $[\frac{h}{3}, \frac{2 \times h}{3}]$ and $[\frac{2 \times h}{3}, h]$ with h the maximum height.

To evaluate the effect of the number and type of laser metrics on prediction accuracy, we tested predictors sets obtained by combination of $(n_h, n_d, n_e) \in (\{0, 4, 6, 8\} \times \{0, 1, 2, 3\} \times \{0, 1, 2, 3\})$. When the number of observations $N = 31$ was greater than the number of variables n_v , PCA and ICA were performed for dimension reduction (DR). PCA is considered one of the most applicable DR method [17]. It reduces dimensionality by extracting from the original data set components which encompass the highest variance. As our data include different variables (heights, densities, entropies), a correlation-PCA was performed, i.e. the original data set was centered and standardized beforehand. Regarding ICA, components are also called latent variables. Their extraction is based on maximization of the statistical independence of the estimated components. We used an implementation of the fastICA algorithm [18]. Subsets of dimension $n_v \in \{1, 2, 3, 4, 5, 6, 8, 10, 12, 14, 16, 18, 20, 22, 24\}$ of the obtained principal and independent components were also used as sets of predictors.

B. Regression methods

For each dependent variable $y \in \{H_{dom}, G, N_s, \overline{dbh}\}$ and each predictors set (v_i) , the resulting training data $\{(x_1, y_1), \dots, (x_N, y_N)\} \subset \mathbf{R}^{n_v} \times \mathbf{R}$ was used to fit a multiple regression model $y = b + \sum_{i=1}^{n_v} a_i \times v_i$ by ordinary least squares, where $(v_i)_{i \in \{1, \dots, n_v\}}$ is a set of predictors and $((a_i)_{i \in \{1, \dots, n_v\}}, b)$ are model parameters. Models including a maximum of three predictors were tested by exhaustive search

among all the possible combinations. Models which did not fulfill the linear model assumptions or including a predictor with a partial p-value greater than 0.05 were discarded. For each predictors set the model with highest adjusted coefficient of determination ($adj-R^2$) was selected.

Data sets were also used to train an ϵ -SVR. It is a common implementation of SVR which aims at approximating a function $f : y = f(v)$ with a solution of the form $f(v) = \sum_{j=1}^n \alpha_j k(v, x_j) + \beta$ that has at most ϵ deviation from the actual targets y_j . $((\alpha_j)_{j \in \{1, \dots, n\}}, \beta)$ are parameters determined during the training process and k a kernel function. Linear $k(x, z) = \langle x, z \rangle$ and radial-basis $k(x, z) = \exp(-\gamma \|x - z\|^2)$ kernels were tested. Hyper parameters C and γ were selected by tuning over a range of pre defined values and selecting the combination which yielded the lowest root mean square error. Cost parameter C is a positive constant that defines the trade off between training error and model flatness. Tested values were $C \in (10^i)_{i=-5, -4, \dots, 3}$. The same range was investigated for radial kernel γ parameter.

Regression models accuracies were evaluated in leave-one-out cross validation by computing the root mean square error $RMSE = \sqrt{\frac{1}{N} \sum_{i=1}^N (y_i - \hat{y}_i)^2}$ (where y_i and \hat{y}_i are the observed and predicted values, and N the number of observations) and its coefficient of variation $CV_{RMSE} = \frac{RMSE}{\bar{y}}$ with $\bar{y} = \frac{1}{N} \sum_{i=1}^N y_i$.

IV. RESULTS

Prediction by *ols*-MR yields satisfactory results. For the predictors set $(n_h, n_d, n_e) = (6, 3, 3)$ with 30 laser metrics without DR, the coefficient of variation of the RMSE ranges from 12.6 to 23.6%. The best result is achieved for dominant

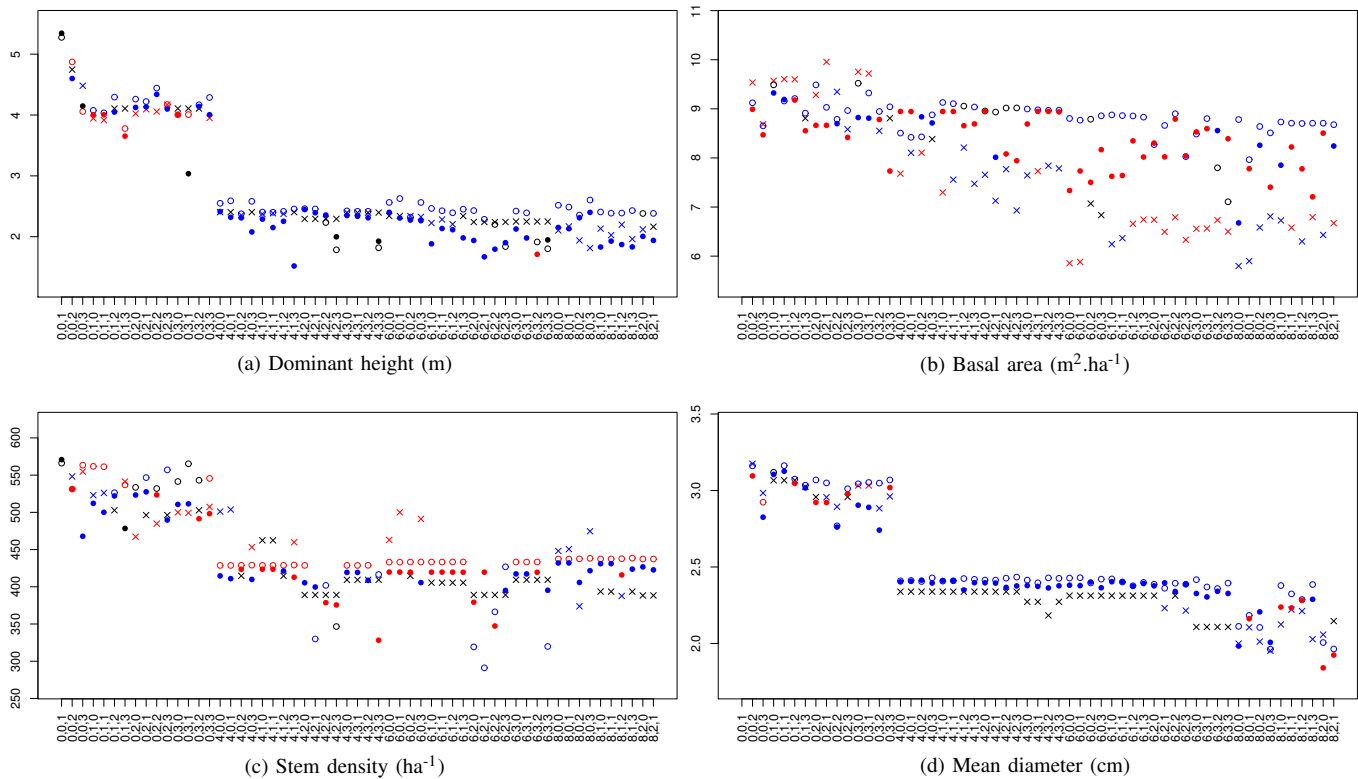


Fig. 4. Influence of the number and type of laser metrics on prediction accuracy (RMSE obtained by leave-one-out cross validation) of *ols*-MR (×) and ϵ -SVR with linear (○) and radial (●) kernels. Triplets on the x-axis refer to the number of laser height, density and entropy metrics (n_h, n_d, n_e) used to construct the predictors sets. Symbol colors refer to the DR method that produced the best accuracy: PCA (blue), ICA (red) or none (black).

height whereas stem density performs poorly. Mean diameter and basal area obtain intermediate values (14.6 and 19.6% respectively). For this predictors set, PCA do not improve models accuracy. ICA performs even worse, except for basal area (18.7%). Table II summarizes the best results obtained with *ols*-MR and ϵ -SVR for the predictors sets derived from $(n_h, n_d, n_e) = (6, 3, 3)$. ϵ -SVR performs better than *ols*-MR for dominant height and stem density. However values are rather close. Fig. 3 illustrates the effect of dimension reduction and kernel selection on ϵ -SVR accuracy for predictors sets derived from $(n_h, n_d, n_e) = (6, 3, 3)$. On the whole, preliminary DR by PCA yields lower prediction error than with ICA, and radial kernel performs better than linear kernel. Besides, ϵ -SVR seems less sensitive to the number of components when PCA is employed instead of ICA. However, for dominant height and basal area, the best accuracy is obtained with a linear kernel and without dimension reduction.

Fig. 4 depicts the influence of the number and type of laser metrics on prediction accuracy. For all forest parameters, accuracy is improved when a minimum number of height metrics are included in the data sets ($n_h \geq 4$). On the whole, the two methods display similar performance, except for basal area. Radial kernel gives slightly better results than linear kernel ϵ -SVR. Optimal DR methods depend on the regression technique used, on the forest parameter and also on the number and type of laser metrics. ϵ -SVR accuracy is generally improved with DR. However, when employed for linear kernel ϵ -SVR, ICA results in poor performance for all stand pa-

rameters except stem density. *ols*-MR performs better on raw laser metrics, except for basal area, or when more than eight height metrics are included in the model for dominant height and mean diameter prediction. Regarding dominant height (Fig. 4a), radial kernel ϵ -SVR combined with PCA gives the best results. Best accuracies with *ols*-MR are obtained with PCA or without DR, depending on the laser metrics included in the predictors. The entropy metrics have a visible effect only for the combination $(n_h, n_e) = (4, 3)$. For basal area (Fig. 4b), results are more scattered. Linear kernel ϵ -SVR performs poorly but stably with PCA. Better but variable accuracies are achieved with radial kernel ϵ -SVR and ICA. *ols*-MR gives the best results, particularly when laser metrics only include height variables $(n_h, n_d, n_e) \in \{6, 8\} \times \{0\} \times \{0, 1\}$. Concerning stem density (Fig. 4c), the two methods also display similar accuracy. Linear kernel ϵ -SVR with ICA remains stable, whereas radial kernel gives better but more variable results. Density metrics have a strong influence on accuracy, particularly for *ols*-MR with $n_d = 2$. Particular combinations of density and entropy metrics $(n_d, n_e) \in \{(2, 1), (3, 3)\}$ yield good accuracies. For mean diameter (Fig. 4d), regression methods yield close results. Except when the data sets include eight height metrics, results are very stable, particularly for ϵ -SVR combined with PCA. Slightly higher accuracies are obtained with multiple regression, especially with $(n_h, n_d) = (6, 3)$. When more height metrics are included, both methods give better but less stable results.

V. DISCUSSION

Multiple regression prediction results are similar to those obtained in a study carried out on 34 deciduous plots located in the Bavarian Forest National Park (Germany) [7]. With our data, ϵ -SVR combined with DR achieves results similar to *ols*-MR and even outperforms it. ϵ -SVR performs best mainly with PCA whereas multiple regression prefers raw data. Acceptable prediction accuracies can be obtained with a limited number of height metrics only ($n_h = 4$). Further improvement thanks to additional laser metrics depends on the considered forest parameter. Indeed, general trends are difficult to interpret. Some clues may be found in physical links between forest attributes and structure. Previous studies [2], [4] showed that dominant height and, to a lesser extent, mean diameter are correlated with the upper height quantiles. This may explain why those stand parameters display similar tendencies regarding prediction models: stability of results when enough height metrics are included in the predictors, and inefficiency of DR for *ols*-MR. Relationships between basal area or stem density and forest structure are more complex, resulting in patterns that are harder to interpret. Besides, the number of samples is quite low with respect to the high variability of forest parameters in the study area. The presence of outliers and the risk of over fitting the ϵ -SVR models are likely to degraded prediction accuracy. The introduced entropy metrics proved to be useful only in some particular cases for dominant height and stem density prediction. They turn out to have no or little effect when more than eight height metrics are already present in the predictors sets.

After extracting laser metrics with an area based method, one may be tempted to process the high dimensional obtained data sets with regression or classification techniques employed for multispectral data, such as SV machines. However, as pointed out in this paper, the choice of metrics to be extracted for the irregularly sampled laser point cloud is not straightforward as variables with relevant information depend on the forest parameter to be estimated. The extraction of a higher number of variables could be a turnaround, but requires more costly field observations for algorithms training. Regarding dimension reduction, combinations of different types of variables (height, density, entropy) may represent an issue for the design of more efficient dimension reduction techniques.

VI. CONCLUSION

The results of the area-based method applied in this study to predict forest parameters from airborne laser scanning data show that the accuracy of ϵ -SVR estimates are similar to those obtained by *ols*-MR. Dimension reduction of laser metrics improves the ϵ -SVR accuracy, whereas *ols*-MR performs better on raw laser metrics. On the whole, radial kernel turns out to be slightly more accurate and robust than linear kernel. *ols*-MR is more sensitive to the number and type of laser variables included in the training sets than ϵ -SVR. Moreover the effect of addition or removal of laser metrics depends on the predicted forest parameter.

Further research should focus on factors that may improve support vector regression, such as other kernels or algorithms

(ν -SVR), and specially designed dimension reduction techniques. Besides advantage could be taken of SVR robustness when predicting parameters for forest stands or laser data different from those used to train the algorithm. The trade-off between accuracy of estimates and intensity of field campaign is indeed a major factor of concern when dealing with forest inventory at operational scale in mountainous areas.

REFERENCES

- [1] S. Magnussen and P. Boudewyn, "Derivations of stand heights from airborne laser scanner data with canopy-based quantile estimators," *Can. J. For. Res.*, vol. 28, no. 7, pp. 1016–1031, 1998.
- [2] J. Holmgren, "Prediction of tree height, basal area and stem volume in forest stands using airborne laser scanning," *Scand. J. For. Res.*, vol. 19, no. 6, pp. 543–553, Dec. 2004.
- [3] K. Lim, P. Treitz, K. Baldwin, I. Morrison, and J. Green, "Lidar remote sensing of biophysical properties of tolerant northern hardwood forests," *Can. J. Remote Sens.*, vol. 29, no. 5, pp. 658–678, Oct. 2003.
- [4] E. Næsset, "Predicting forest stand characteristics with airborne scanning laser using a practical two-stage procedure and field data," *Remote Sens. Environ.*, vol. 80, no. 1, pp. 88–99, Apr. 2002.
- [5] E. Næsset, T. Gobakken, J. Holmgren, H. Hyyppä, J. Hyyppä, M. Maltamo, M. Nilsson, H. Olsson, A. Persson, and U. Söderman, "Laser scanning of forest resources: the Nordic experience," *Scand. J. For. Res.*, vol. 19, no. 6, pp. 482–499, Dec. 2004.
- [6] S. C. Popescu, R. H. Wynne, and R. F. Nelson, "Estimating plot-level tree heights with lidar: local filtering with a canopy-height based variable window size," *Comput. Electron. Agric.*, vol. 37, no. 1-3, pp. 71–95, Dec. 2002.
- [7] M. Heurich and F. Thoma, "Estimation of forestry stand parameters using laser scanning data in temperate, structurally rich natural european beech (*fagus sylvatica*) and norway spruce (*picea abies*) forests," *Forestry*, vol. 81, no. 5, pp. 645–661, Apr. 2008.
- [8] E. Næsset, O. M. Bollandsås, and T. Gobakken, "Comparing regression methods in estimation of biophysical properties of forest stands from two different inventories using laser scanner data," *Remote Sens. Environ.*, vol. 94, no. 4, pp. 541–553, Feb. 2005.
- [9] P. Packalén and M. Maltamo, "The k-MSN method for the prediction of species-specific stand attributes using airborne laser scanning and aerial photographs," *Remote Sens. Environ.*, vol. 109, no. 3, pp. 328–341, Aug. 2007.
- [10] H. Niska, J. P. Skön, P. Packalén, T. Tokola, M. Maltamo, and M. Kolehmainen, "Neural networks for the prediction of species-specific plot volumes using airborne laser scanning and aerial photographs," *IEEE Trans. Geosci. Remote Sens.*, vol. 48, no. 3, pp. 1076–1085, Mar. 2010.
- [11] T. Hastie, R. Tibshirani, and J. H. Friedman, *The Elements of Statistical Learning*, corrected ed. Springer, July 2003.
- [12] G. Licciardi, F. Pacifici, D. Tuija, S. Prasad, T. West, F. Giacco, C. Thiel, J. Inglada, E. Christophe, J. Chanussot, and P. Gamba, "Decision fusion for the classification of hyperspectral data: Outcome of the 2008 GRS-S data fusion contest," *IEEE Trans. Geosci. Remote Sens.*, vol. 47, no. 11, pp. 3857–3865, Nov. 2009.
- [13] H. Zhan, P. Shi, and C. Chen, "Retrieval of oceanic chlorophyll concentration using support vector machines," *IEEE Trans. Geosci. Remote Sens.*, vol. 41, no. 12, pp. 2947–2951, Dec. 2003.
- [14] D. Sun, Y. Li, and Q. Wang, "A unified model for remotely estimating chlorophyll a in lake Taihu, China, based on SVM and in situ hyperspectral data," *IEEE Trans. Geosci. Remote Sens.*, vol. 47, no. 8, pp. 2957–2965, Aug. 2009.
- [15] G. Moser and S. B. Serpico, "Modeling the error statistics in support vector regression of surface temperature from infrared data," *IEEE Geosci. Remote Sens. Lett.*, vol. 6, no. 3, pp. 448–452, Jul 2009.
- [16] G. Camps-Valls, J. Munoz-Mari, L. Gomez-Chova, K. Richter, and J. Calpe-Maravilla, "Biophysical parameter estimation with a semisupervised support vector machine," *IEEE Geosci. Remote Sens. Lett.*, vol. 6, no. 2, pp. 248–252, Apr. 2009.
- [17] R. Dianat and S. Kasaei, "Dimension reduction of optical remote sensing images via minimum change rate deviation method," *IEEE Trans. Geosci. Remote Sens.*, vol. 48, no. 1, pp. 198–206, Jan. 2010.
- [18] A. Hyvärinen, "Fast and robust fixed-point algorithms for independent component analysis," *IEEE Trans. Neural Netw.*, vol. 10, no. 3, pp. 626–634, May 1999.